Computational Study on the Kinetics and Mechanisms for the HCO + O3 Reaction

ARTICLE *in* THE JOURNAL OF PHYSICAL CHEMISTRY A · APRIL 2014

Impact Factor: 2.69 · DOI: 10.1021/jp4127013 · Source: PubMed

4 AUTHORS, INCLUDING:

Hsin-Tsung Chen

Chung Yuan Christian University

78 PUBLICATIONS **704** CITATIONS

THE JOURNAL OF PHYSICAL CHEMISTRY A

Article

pubs.acs.org/JPCA

Computational Study of the Kinetics and Mechanisms for the HCO + O_3 Reaction

Chen-Chi Lee, Mei-Ya Lin, Yu-Huan Lu, and Hsin-Tsung Chen*

Department of Chemistry and Center for Nanotechnology, Chung Yuan Christian University, Chungli 32023, Taiwan

ABSTRACT: The mechanisms of radical−molecule reactions between HCO (formyl radical) and O_3 (ozone) have been investigated by using BH&HLYP and QCISD methods with the 6-311++G(3df,2p) basis set. The energetics have been refined with CCSD(T) and QCISD(T) theoretical approaches with the same basis set based on the geometries calculated at the QCISD method. The intermediates of hydrogen-bonded complexes and the critical transition states are also examined with the multireference methods. Two possible reaction pathways containing hydrogen-abstraction and association−elimination processes for the interaction of HCO with O_3 are proposed. Both reaction mechanisms can occur via the prereactive hydrogen-bonded complex, O_3−HCO, with 2.45 kcal/mol stability at the CCSD(T) approach with respect to the reactants; even so, the hydrogen-abstraction mechanism exhibits a lower energy barrier. The rate constants for both processes are also predicted. The total rate constant at 298 K is calculated to be in close agreement with the experimental value of 8.3×10^{-13} cm^3 $molecule^{-1}$ s^{-1}.

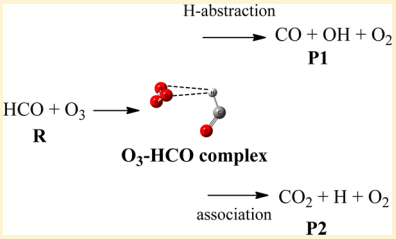

INTRODUCTION

The formyl radical (HCO) is a crucial species in the oxidation of hydrocarbon combustion and in tropospheric chemistry.[1,2] To model the HCO radicals chemistry of the combustion and atmosphere, numerous reactions concerning HCO with O_2,[3,4] NO,[3−6] NO_2,[4,7−9] and Cl_2[4,10] have been studied by the experiment and theory. The radical−molecule reaction of HCO with ozone may be of great importance in the ozone-destruction process.[11] Understanding their key roles in atmospheric and combustion chemistry needs knowledge of their reactivity and details of reaction mechanisms. To our best knowledge, the mechanism of this reaction has not yet been fully characterized. The reaction of HCO + O_3 may take place as the following possible channels

$$HCO + O_3 \rightarrow HCO_2 + O_2 \rightarrow H + CO_2 + O_2 \quad (1)$$

$$\rightarrow HO_3 + CO \rightarrow HO + O_2 + CO \quad (2)$$

The existing mechanism assumed HCO_2 + O_2 via an association−elimination process as the major products, which give H + CO_2 + O_2, while HO_3 + CO were assumed via a hydrogen-abstraction process as the minor products that generate OH + O_2 + CO. Although the former channel is more exothermic than the latter, we believe that the latter may be more important. The rate constant of the HCO + O_3 reaction measured by Atkinson et al.[11] is quite low, about 8.3×10^{-13} cm^3 $molecule^{-1}$ s^{-1} at 298 K. The lack of rate constant data for the HCO + O_3 reaction makes its mechanisms unclear. We propose that a prereactive hydrogen-bonded complex would be formed between HCO and O_3 at the first stage of the reaction, similar to the systems of O_3 and HO, HO_2, or HNO.[12−15] The existing prereactive hydrogen-bonded complex has been found to play an important role in interpreting the kinetic behavior in many atmospheric reactions.[12−16] Understanding the kinetics and mechanism of the title reaction is therefore crucial to dependably model atmospheric O_3 phenomena.[17,18]

As we know, theoretical studies of the reaction mechanism and the potential energy surface have not been reported. In this work, our aim is to seek the possible potential energy surface and the prereactive hydrogen-bonded complex of the radical−radical interaction between HCO and O_3 by using high-level molecular orbital calculations. Referring to the theoretical studies on the similar reaction of HO_2 + O_3,[14,19,20] the multireference methods including CASSCF and CASPT2 are carried out to characterize the hydrogen-bonded complexes and the critical transition states. Such studies could supply useful information for the chemical kinetic analysis. In addition, we also calculated the rate constants for both reaction channels by the variational transition-state theory (TST) and/or Rice−Ramsperger−Kassel−Marcus (RRKM) theory.[21]

COMPUTATIONAL METHODS

All geometries of stationary points including reactants, intermediates, products, and transition states have been optimized by employing the 6-311++G(3df, 2p) basis set.[22,23] In a first step, we carried out density functional theory with the BH&HLYP[24] level to locate all stationaries of the potential energy surfaces (PESs). The BH&HLYP method has been employed in previous work[15] on the reaction of HO_2 + O_3, demonstrating that the BH&HLYP method gives accurate results. In order to confirm the hydrogen-bonded complexes and critical transition states, the QCISD approch[25] with the 6-311++G(3df,2p) basis set has been used to reoptimize and characterize their structures in a second step. The stationary

Received: December 27, 2013
Revised: April 14, 2014
Published: April 16, 2014

dx.doi.org/10.1021/jp4127013 | J. Phys. Chem. A 2014, 118, 3395−3401

Table 1. Calculated and Experimental Heat of Formation of HCO + O_3[a]

		ΔH (kcal/mol)						
reaction		BH&HLYP	QCISD(T)// BH&HLYP	CCSD(T)// BH&HLYP	QCISD	QCISD(T)// QCISD	CCSD(T)// QCISD	exp.
HCO + O_3→	H + CO_2 + O_2	−112.13	−82.91	−82.98	−100.51	−82.36	−82.43	−85.84
	HO + O_2 + CO	−93.33	−67.42	−68.00	−79.28	−65.84	−67.32	−62.80

[a]The unit of energy is kcal/mol. All calculations are carried out by using the 6-311++G(3df,2p) basis set.

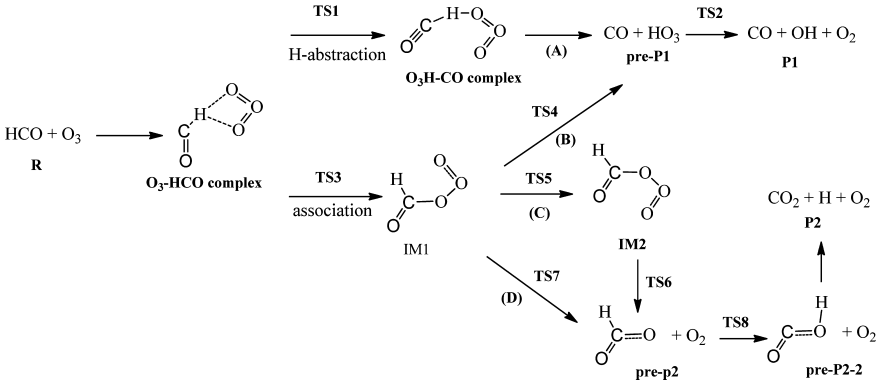

Figure 1. The possible reaction pathways of HCO + O_3 are characterized into four different parts, A, B, C, and D.

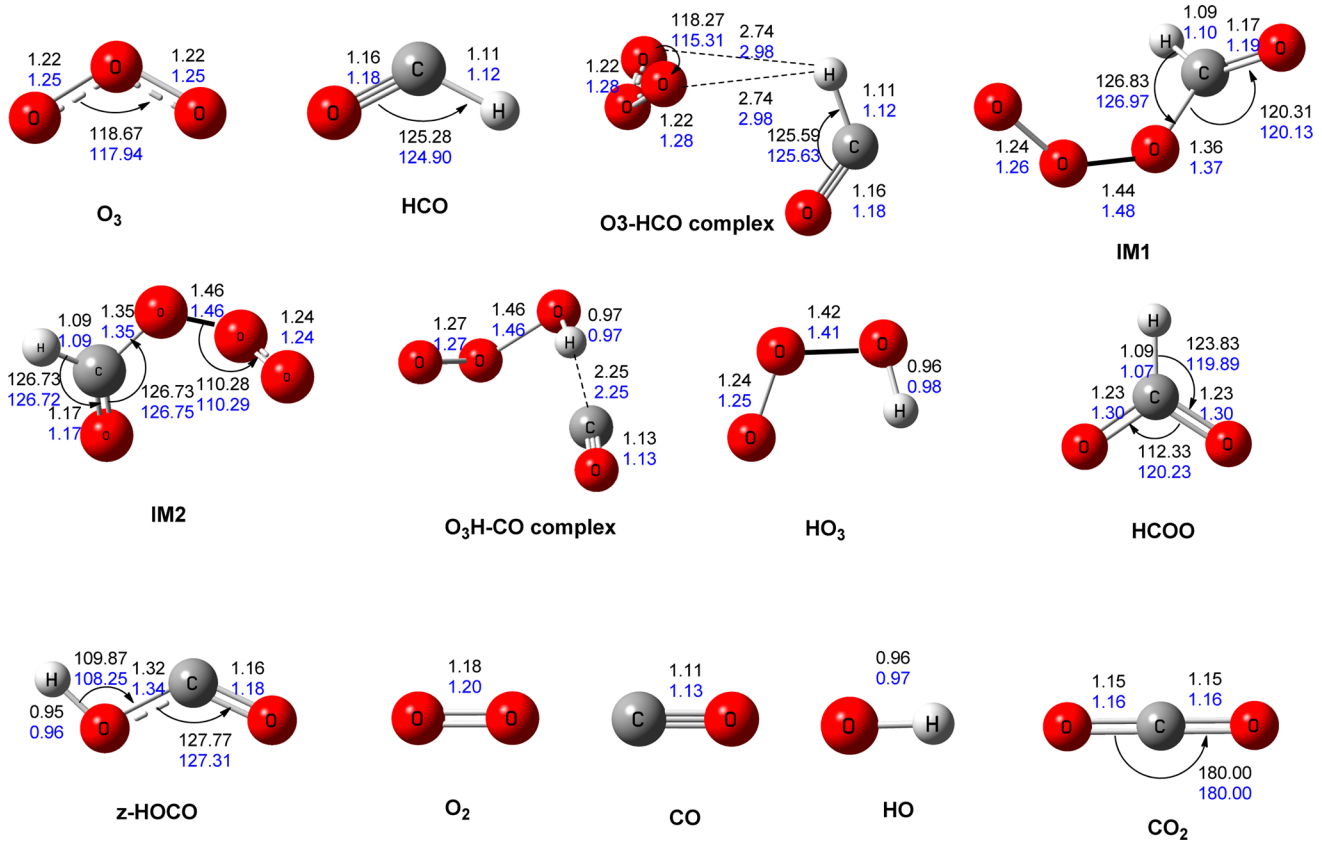

Figure 2. The optimized geometries of the possible intermediates and products calculated at the BH&HLYP and QCISD levels with the 6-311++G(3df,2p) basis set. Bond lengths are given in Å and angles in degrees. The parameters in black and blue are BH&HLYP and QCISD, respectively.

points were characterized with vibrational frequency calculations at the same method. The stationaries with positive vibrational frequencies (number of imaginary frequencies; NIMAG = 0) were identified for local minima, while those with NIMAG = 1 were assigned to saddle points. The intrinsic reaction coordinate (IRC)[26] calculations were performed to confirm the transition structures connecting designated intermediates. For the diradical character of the reactant O_3 with the $^1A'$ ground electronic state and the O_2 product with the $^3\Sigma_g$ triplet ground state, the mixing doublet−quatet wave function was employed for the doublet PES of the HCO + O_3 reaction. To obtain reliable energies, we carried out single-point

dx.doi.org/10.1021/jp4127013 | J. Phys. Chem. A 2014, 118, 3395−3401

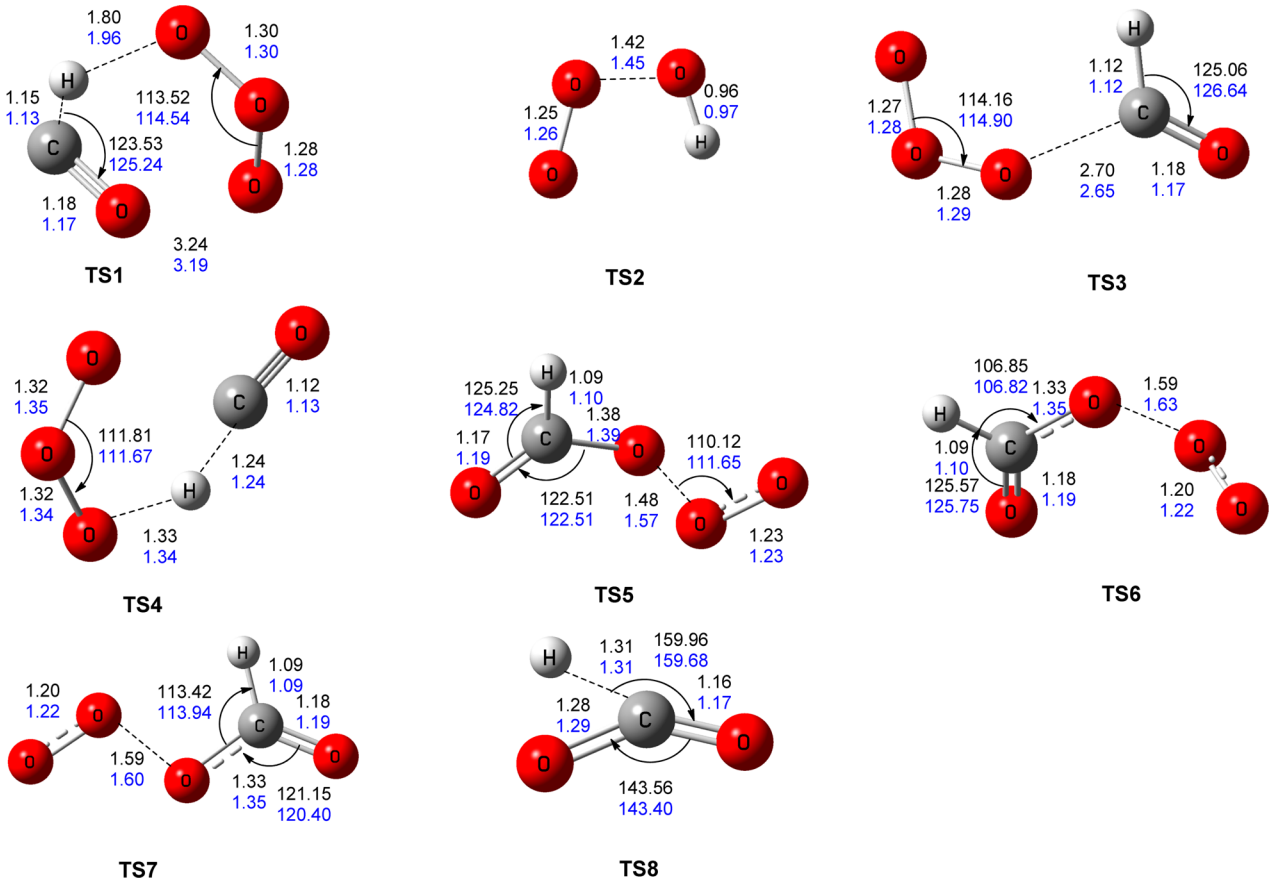

Figure 3. The optimized geometries of the transition states calculated at the BH&HLYP and QCISD levels with the 6-311++G(3df,2p) basis set. Bond lengths are given in Å and angles in degrees. The parameters in black and blue are BH&HLYP and QCISD, respectively.

calculations by using the CCSD(T)[27] and QCISD(T) methods based on the geometries located at both BH&HLYP and QCISD methods. The highest levels of theory obtained in this work are thus denoted as CCSD(T)//BH&HLYP, CCSD(T)//QCISD, QCISD(T)//BH&HLYP, and QCISD(T)//QCISD. We also considered the value of the T1 diagnostic[28,29] of QCISD(T) and CCSD(T) wave functions to estimate the reliability of those calculations with regard to the wave function with multireference character. The single determinant wave function nature of all calculated structures was verified by executing T1 diagnostics (the T1 parameter is predicted to be in the region of 0.02−0.06). In addition, multiconfigurational effects on the energies of some species in the PES are examined. Their geometries were reoptimized at the CASSSCF(11,11)/6-311++G(3df, 2p) method.[30−32] On the basis of the geometries from this method, single-point calculations were carried out with the CASPT2 level[33−36] with the same basis set.

RESULTS AND DISCUSSION

Computational Condition Tests. The calculated and experimental[37] heats of formation of HCO + O_3 → H + CO_2 + O_2 and HCO + O_3 → HO + O_2 + CO are presented in Table 1. The heats of formation computed by the QCISD(T)//QCISD and CCSD(T)//QCISD methods with a 6-311++G(3df,2p) basis set are −82.36 and −82.43 kcal/mol for the reaction of HCO + O_3 → H + CO_2 + O_2 and −65.84 and −67.32 kcal/mol for the reaction of HCO + O_3 → HO + O_2 + CO, which are both in satisfactory agreement with experimental values (−85.84 and −62.80 kcal/mol),[37] whereas the calculated BH&HLYP energy, −112.13 and −93.33 kcal/mol, substantially overestimates the experimental value. Interestingly, the calculated heats of formation at the CCSD(T)//BH&HLYP energy, −82.98 and −68.00 kcal/mol, are in good agreement with the experimental values and the higher-level CCSD(T)//QCISD energy. It should be noted that the values calculated with the QCISD(T)//QCISD and CCSD(T)//QCISD methods are around 3−5 kcal/mol higher than those of experiment. The limited basis set may give rise to the deviations; unfortunately, QCISD calculation with a larger basis set is not feasible. However, the structures of hydrogen-bonded complexes and the critical transition states are more properly described by the singe-determinant-based QCISD approach.[14] Accordingly, we choose the QCISD(T)//QCISD and CCSD(T)//QCISD methods to map out the PES of the title reaction.

Reaction Mechanisms and PES of the HCO + O_3 Reaction. There are two possible reaction pathways containing hydrogen-abstraction and association−elimination processes for the interaction of HCO with O_3, as alluded to in the Introduction. As depicted in Figure 1, the considered reaction can progress in four channels, A−D, leading to two possible product formation mechanisms. The intermediates and pre-products are correspondingly named IM1, IM2, pre-P1, pre-P2, and pre-P2-2 and the products, HO + O_2 + CO and H + CO_2 + O_2, are described as P1 and P2, respectively. The transition states connecting two intermediates are denoted as TS1−TS8. The optimized structures of the intermediates and transition

dx.doi.org/10.1021/jp4127013 | J. Phys. Chem. A 2014, 118, 3395−3401

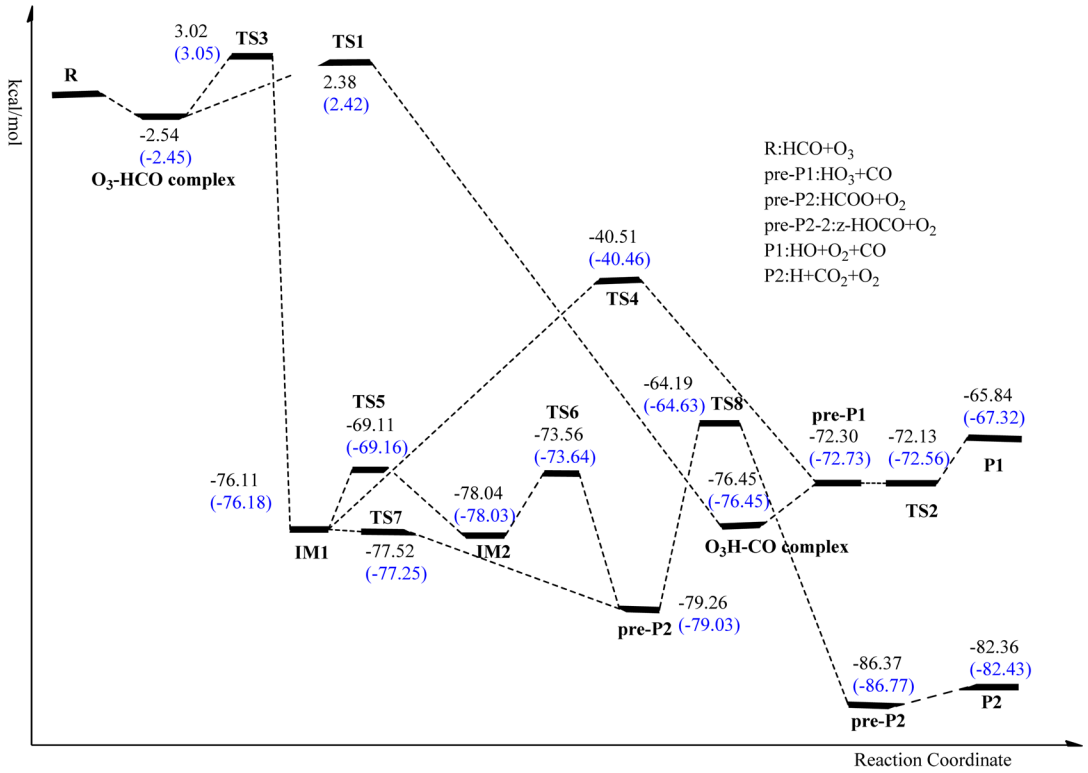

Figure 4. The PESs for the pathways of the HCO + O_3 reaction leading to the products P1 and P2 calculated at the CCSD(T)//QCISD and QCISD(T)//QCISD levels with ZPE correction. The values in parentheses are CCSD(T)//QCISD energies.

states calculated with the BH&HLYP/6-311++G(3df,2p) and QCISD/6-311++G(3df, 2p) methods are depicted in Figures 2 and 3, respectively. Figure 4 shows the predicted PESs at the CCSD(T)/6-311++G(3df, 2p)//QCISD/6-311++G(3df, 2p) and QCISD(T)/6-311++G(3df, 2p)//QCISD/6-311++G(3df, 2p) levels. Relative energies with zero-point vibration energy (ZPE) correction of intermediates, transition states, and products with respect to the reactants (HCO + O_3) are listed in Table 2.

As seen in Figure 4, the reaction proceeds via two different mechanisms, called the hydrogen-abstraction and association−elimination mechanisms. The first step of both mechanisms takes place by the attachment of O_3 to the H atom of HCO to form a prereactive hydrogen-bonded complex via weak van der Waals forces, O_3−HCO, whose energies at QCISD, QCISD(T)//QCISD, and CCSD(T)//QCISD levels with ZPE correction are 4.53, 2.54, and 2.45 kcal/mol below the reactants HCO + O_3. The lengths of hydrogen bonds in O_3−HCO are predicted to be 2.74 and 2.98 Å at BH&HLP and QCISD levels, respectively. The calculated T1 diagnostic values of the O_3−HCO hydrogen-bonded complex at the QCISD and CCSD(T) levels are 0.05, which are in the range of the values reported by Rienstra-Kiracofe et al.[29] As alluded to above, the reaction may occur via two different mechanisms starting from the O_3−HCO hydrogen-bonded complex, (a) hydrogen-abstraction and (b) association−elimination mechanisms.

(a) The hydrogen-abstraction mechanism. From the O_3−HCO hydrogen-bonded complex, it undergoes a hydrogen-abstraction channel by passing through TS1 to produce the hydrogen-bonded complex, O_3H−CO. The breaking H−C and forming H−O lengths in TS1 are calculated to be 1.13 (1.15) and 1.96 (1.80) Å at the QCISD (BH&HLP) level. The relative energies of TS1 are calculated to be −4.36, 2.38, and 2.42 kcal/mol at QCISD, QCISD(T)//QCISD, and CCSD(T)//QCISD levels. The dissociation of HO_3 proceeds by breaking the O−O bond via TS2 to form the product of OH + O_2. The breaking O−O bond in TS2 is calculated to be 1.45 (1.42) Å at the QCISD (BH&HLP) level. The barrier for the O−O cleavage

Table 2. ZPE (kcal/mol) and Relative Energies (RE, kcal/mol) of Reactants, Intermediates, Transition States, and Products Calculated at the QCISD (QRE), QCISD(T)//QCISD (QTRE/Q), and CCSD(T)//QCISD (CTRE/Q) Levels with the 6-311++G(3df,2p) Basis Set

species	ZPE[a]	QRE +ZPE[b]	QTRE/Q +ZPE[b]	CTRE/Q +ZPE[b]
R	12.64	0.00	0.00	0.00
IM1	17.77	−68.82	−76.11	−76.18
IM2	17.77	−73.72	−78.04	−78.03
O_3−HCO complex	13.10	−4.53	−2.54	−2.45
O_3H−CO complex	15.54	−74.23	−76.44	−76.45
pre-P1	14.63	−73.38	−72.13	−72.56
pre-P2	14.95	−84.42	−79.26	−79.03
pre-P2-2	15.76	−100.44	−86.37	−86.77
TS1	13.16	−4.36	2.38	2.42
TS2	14.46	−73.38	−72.30	−72.73
TS3	13.10	−4.00	3.02	3.05
TS4	17.29	−30.63	−31.40	−39.78
TS5	16.76	−62.99	−69.11	−69.16
TS6	16.67	−74.12	−73.56	−83.64
TS7	17.21	−69.67	−77.52	−77.25
TS8	11.69	−64.13	−64.19	−64.63
P1	10.94	−79.28	−65.84	−67.32
P2	9.80	−100.51	−82.36	−82.43

[a]ZPE (kcal/mol) at the QCISD/6-311++G(3df,2p) level. [b]Relative energy (kcal/mol) with respect to the reactants.

dx.doi.org/10.1021/jp4127013 | J. Phys. Chem. A 2014, 118, 3395−3401

through TS2 is only 0.17 kcal/mol at the QCISD(T) level. It should be note that the energy of TS2 is lower than the product, P1 (HO + O_2 + CO), at both QCISD(T) and CCSD(T) levels, whereas it is higher at the BH&HLP level. The entire reaction process A, HCO + O_3 → O_3−HCO → TS1 → O_3H−CO → pre-P1 → TS2 → CO + OH + O_2, is calculated to be exothermic by 65.84 and 67.32 kcal/mol at the QCISD(T)//QCISD and CCSD(T)//QCISD levels, respectively, which agree with the experimental value of 62.80 kcal/mol.[37]

(b)The association−elimination mechanism. In the second pathway, the reaction also occurs starting from the prereactive hydrogen-bonded complex, O_3−HCO. Then, O_3 and HCO undergo the O−C bond addition via TS3 to form the IM1, which has a *cis*-HCOO structure as shown in Figure 3. The IM1 intermediate is calculated to be −76.11 and −76.18 kcal/mol with respect to the reactants at the QCISD(T)//QCISD and CCSD(T)//QCISD levels. The relative energies of TS3 are −4.00, 3.02, and 3.05 kcal/mol, respectively, at the QCISD, QCISD(T)//QCISD, and CCSD(T)//QCISD levels. The forming C−O lengths in TS3 are calculated to be 2.65 (2.70) Å at the QCISD (BH&HLP) level. As the reaction proceeds, the IM1 intermediate may undergo three reorganization pathways, B−D. From the IM1 intermediate, the first pathway B occurs by transferring the H atom bonded to the C atom to the O atom and simultaneously by breaking the O−C bond to form HO_3 + CO, pre-P1, via TS4, passing a high barrier of 36.60 and 35.72 kcal/mol, respectively, at the QCISD(T)//QCISD and CCSD(T)//QCISD levels. The forming H−O and breaking O−C in TS4 are calculated to be 1.34 (1.33) and 1.24 (1.24) Å at the QCISD (BH&HLP) level. Then, breaking the O−O bond of HO_3 via TS2 forms the final product of CO + OH + O_2. The entire reaction process B is HCO + O_3 → O_3−HCO → TS3 → IM1 → TS4 → pre-P1 → CO + OH + O_2. The second pathway C occurs by isomerization via TS5 to form the *trans*-HCOO structure, IM2, which is slightly more stable than the cis structure IM1 by 1.93 and 1.85 kcal/mol at the QCISD(T)//QCISD and CCSD(T)//QCISD levels. The barrier of isomerization IM1 → IM2 is computed to be about 7.0 kcal/mol. The reaction proceeds by breaking the O−O bond of the IM2 via TS6, overcoming a barrier of 4.4 kcal/mol to form HCOO + O_2, pre-P2. The breaking O−O bond in TS6 is calculated to be 1.63 (1.59) Å at the QCISD (BH&HLP) level. The relative energies of TS5 and TS6 are 69.11 (69.16) and 73.56 (73.64) kcal/mol at the QCISD(T)//QCISD (CCSD(T)//QCISD) level. The O(H)CO species of pre-P2 undergoes further H migration by passing a barrier (TS8, 15.07 and 14.40 kcal/mol at the QCISD(T)//QCISD and CCSD(T)//QCISD levels) to form HOCO + O_2, pre-P2-2, with an exothermicity of 7.11 (7.74) kcal/mol at the QCISD(T)//QCISD (CCSD(T)//QCISD) level. Finally, the pre-P2-2 might proceed through H−O bond dissociation, forming P2 (H + CO_2 + O_2) without a barrier. The entire reaction process C is HCO + O_3 → O_3−HCO → TS3 → IM1 → TS4 → IM2 → TS6 → pre-P2 → TS8 → pre-P2-2 → CO + OH + O_2, with overall exothermicities of 65.84 and 67.32 kcal/mol, respectively, at the QCISD(T)//QCISD and CCSD(T)//QCISD levels. The third pathway D proceeds by breaking the O−O bond of the IM1 by passing TS7 to form HCOO + O_2, pre-P2. The entire reaction process D is HCO + O_3 → O_3−HCO → TS3 → IM1 → TS7→ pre-P2 → TS8 → pre-P2-2 → CO + OH + O_2.

Multireference Computations. Some of the critical species on the PES are examined with the multiconfigurational effects, as mentioned above. The multireference methods including CASSCF(11,11) and CASPT2 with the 6-311++G(3df, 2p) basis set are carried to characterize the hydrogen-bonded complexes and the critical transition states. The relative energies computed by the CASSCF(11,11) and CASPT2 methods compared with those calculated at the QCISD(T) and CCSD(T) methods are summarized in Table 3. As shown as in Table 3, the calculated relative energies of the hydrogen-bonded complex, O_3−HCO, are −1.94 and −2.38 kcal/mol at the CASSCF(11,11) and CASPT2 methods, which are slightly higher than those obtained by the QCISD(T) and CCSD(T) levels. For the O_3H−CO complex, the predicted relative energies are 7.02 and 11.20 kcal/mol lower than that at the CCSD(T) method. For the transition states, the barriers of TS1 predicted by the CASSCF(11,11) and CASPT2 methods are 3.62 and 1.71 kcal/mol, while the barriers of TS3 are calculated to be 5.74 and 3.36 kcal/mol, respectively. The exothermicities for the formation of P1 and P2 calculated at the CASSCF-(11,11) method are −73.54 and −94.92 and −69.91 and −90.34 kcal/mol at the CASPT2 method. The energies for formation of P1 and P2 by both CASSCF(11,11) and CASPT2 methods are much more than those at the CCSD(T) level or the experimental values. If we use the experimental exothermicities for the formation of P1 and P2, the calculated reaction energies at the CCSD(T) are more reasonable. Accordingly, the rate constant calculations below are carried out based on the CCSD(T) method.

Table 3. Relative Energies (ZPE-Corrected, in kcal/mol) of the Hydrogen-Bonded Complexes and the Critical Transition States on The PES Calculated at the QCISD(T), CCSD(T), CASSCF(11,11), and CASPT2 Levels with the 6-311++G(3df,2p) Basis Set

species	QCISD(T)	CCSD(T)	CASSCF(11,11)	CASPT2
HCO + O_3	0.00	0.00	0.00	0.00
O_3−HCO complex	−2.54	−2.45	−1.94	−2.38
O_3H−CO complex	−76.44	−76.45	−83.47	−87.65
TS1	2.38	2.42	3.62	1.71
TS3	3.02	3.05	5.74	3.36
P1	−65.84	−67.32	−73.54	−69.91
P2	−82.36	−82.43	−94.42	−90.34

Rate Constant Calculations. The rate constants for the reaction occurring by the following product pathways

$$HCO + O_3 \rightarrow O_3{-}HCO \rightarrow HO + O_2 + CO \text{ (via TS1)} \qquad (R_{CO})$$

$$HCO + O_3 \rightarrow O_3{-}HCO \rightarrow H + CO_2 + O_2 \text{ (via TS3)} \qquad (R_{CO_2})$$

have been predicted at 200−1000 K according to the CCSD(T)//QCISD energetics and QCISD molecular parameters by the variational TST and/or RRKM theory implementing the VariFlex code.[21] The multiple reflections effect is introduced because this mechanism is included in a molecular complex with a small well. The barrierless association minimum-energy pathway is approximately described by the Morse potential function, $V(R) = D_e\{1 - \exp[-\beta(R - R_0)]\}^2$, where R is the reaction coordinate, R_0 is the equilibrium O−H bond length, and D_e is the bonding energy without ZPE corrections. The three parameters of the function are R_0 = 2.98 Å, β = 2.86 Å^{-1}, and D_e = 3.52 kcal/mol for HCO + O_3 → O_3−

dx.doi.org/10.1021/jp4127013 | J. Phys. Chem. A 2014, 118, 3395−3401

HCO. In addition, the 1.00 and 80.00 cm^{-1} energy grain sizes are chosen for the convolution of the conserved mode vibrations and for the generation of the transitional-mode number of states, respectively. The transitional-mode contribution to the transition-state number of states for a given energy is estimated by Monte Carlo integration with 10000 configuration numbers. The energy-transfer process was calculated based on the exponential down model with a $\langle \Delta E \rangle_{down}$ value of 400 cm^{-1} for Ar. A 120 cm^{-1} energy grain size was performed to achieve the convergence in the integration over the energy range. The *E,J*-resolved calculation was carried out with the total angular momentum *J* covering the range from 1 to 250 in steps of 10. The multichannel models were performed for the rate constant calculations.

The predicted values for individual rate constants (k_{CO}, k_{CO_2}) and total rate constants ($k_{total} = k_{CO} + k_{CO_2}$) for the HCO + O_3 reaction at an Ar pressure of 100 Torr in the range of 200−1000 K are depicted in Figure 5a. As one can see from Figure 5a, the values of k_{CO}, k_{CO_2}, and k_{total} substantially increase as the temperature increases from 200 to 1000 K. The predicted total rate constant at 298 K is well in agreement with an experimental value of 8.3 × 10^{-13} cm^3 $molecule^{-1}$ s^{-1};[11] see Figure 5a. The calculated rate constants for k_{CO}, k_{CO_2}, and k_{total} can be fitted in the range of 200−1000 K to the three-parameter Arrhenius equations

$$K_{CO} = 2.42 \times 10^{-13} T^{1.82} \exp\left(\frac{-3.32\ \text{kcal/mol}}{RT}\right)\ \text{cm}^3\ \text{molecule}^{-1}\ \text{s}^{-1}$$

$$k_{CO_2} = 1.03 \times 10^{-11} T^{0.56} \exp\left(\frac{-4.08\ \text{kcal/mol}}{RT}\right)\ \text{cm}^3\ \text{molecule}^{-1}\ \text{s}^{-1}$$

$$k_{total} = 1.52 \times 10^{-12} T^{0.92} \exp\left(\frac{-3.58\ \text{kcal/mol}}{RT}\right)\ \text{cm}^3\ \text{molecule}^{-1}\ \text{s}^{-1}$$

Figure 5b, displays the calculated branching ratio for CO and CO_2 products in the range of 200−1000 K. With increasing temperature, the branching ratio for the CO product decreases from 72 to 55%, while that for the CO_2 product increases from 28 to 45%. However, the dominant reaction channel is HCO + O_3 → HO_3 + CO → HO + O_2 + CO.

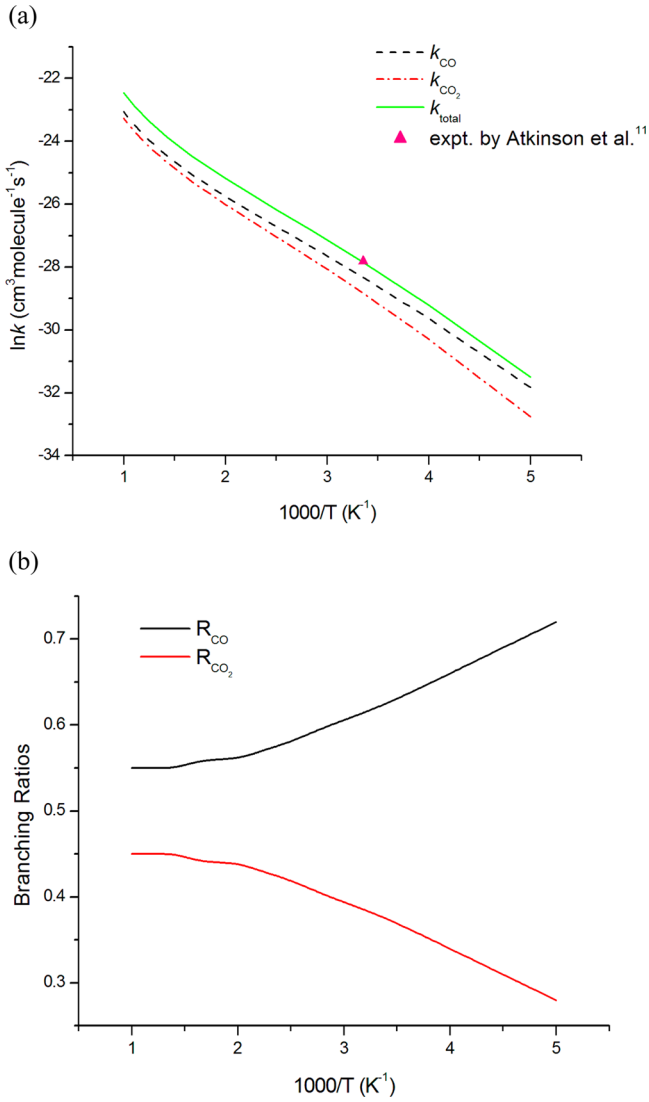

Figure 5. (a) Predicted rate constants of individual rate constants (k_{CO}, k_{CO_2}) and total rate constants ($k_{total} = k_{CO} + k_{CO_2}$) for the reaction of HCO + O_3 at 100 Torr of Ar pressure in the temperature range of 200−1000 K. (b) The predicted branching ratio for CO and CO_2 products in the temperature range of 200−1000 K.

CONCLUSION

The configurations of the reactants, intermediates, transition states, and products as well as the mechanisms of radical−molecule reactions between HCO and ozone have been investigated at the BH&HLYP/6-311++G(3df,2p) and QCISD/6-311++G(3df,2p) levels of theory. To gain reliable energies, we carried out single-point calculations by employing the CCSD(T) and QCISD(T) levels for those structures optimized at the QCISD level. Two possible reaction mechanisms containing hydrogen-abstraction and association−elimination processes for the interaction of HCO with O_3 are found. Both reaction mechanisms can take place via the prereactive hydrogen-bonded complex, O_3−HCO, which is 2.45 kcal/mol at the CCSD(T) level lower than the reactants. The barriers for hydrogen-abstraction and association−elimination processes are computed to be 4.87 and 5.50 kcal/mol at the CCSD(T)//QCISD level, respectively. According to our calculations, the HO_3 + CO via the hydrogen-abstraction process as major products generate OH + O_2 + CO, while the HCO_2 + O_2 via the association−elimination process as minor products give H + CO_2 + O_2. The predicted total rate constant at 298 K agrees well with an experimental value of 8.3 × 10^{-13} cm^3 $molecule^{-1}$ s^{-1}. Some of the crucial species, such as the hydrogen-bonded complexes and the critical transition states on the PES, are also examined with the multireference methods. Compared to the experimental exothermicities, the energies at CCSD(T) seem to be reasonable.

AUTHOR INFORMATION

Corresponding Author

*E-mail: htchen@cycu.edu.tw. Tel:+886-3-265-3324.

Notes

The authors declare no competing financial interest.

ACKNOWLEDGMENTS

H.-T.C. is grateful for (1) the financial support from the Ministry of Science and Technology, Taiwan, under Grant Number NSC 101-2113-M-033-009-MY3 and NSC 101-2632-M-033-001-MY2 and (2) the computer time and facilities from

the National Center for High-performance Computing (NCHC), Taiwan. In addition, we are deeply thankful to Professor M. C. Lin from NCTU, Taiwan, and Emory University, U.S.A. for persistent encouragement and instruction.

REFERENCES

(1) Okabe, H. *Photochemistry of Small Molecules*; Wiley: New York, 1978.
(2) Westbrook, C. K.; Dryer, F. L. *18th International Symposium on Combustion*; The Combustion Institute: Pittsburgh, PA, 1981.
(3) Nesbitt, F. L.; Gleason, J. F.; Stief, L. J. Temperature Dependence of the Rate Constant for the Reaction HCO + O_2 → HO_2 + CO at T = 200−398 K. *J. Phys. Chem. A* **1999**, *103*, 3038−3043.
(4) Ninomiya, Y.; Goto, M.; Hashimoto, S.; Kagawa, Y.; Yoshizawa, K.; Kawasaki, M.; Wallington, T. J.; Hurley, M. D. Cavity Ring-Down Spectroscopy and Relative Rate Study of Reactions of HCO Radicals with O_2, NO, NO_2, and Cl_2 at 295 K. *J. Phys. Chem. A* **2000**, *104*, 7556−7564.
(5) Langford, A. O.; Moore, C. B. Collision Complex Formation in the Reactions of Formyl Radicals with Nitric Oxide and Oxygen. *J. Chem. Phys.* **1984**, *80*, 4211−4221.
(6) Langford, A. O.; Moore, C. B. Reaction and Relaxation of Vibrationally Excited Formyl Radicals. *J. Chem. Phys.* **1984**, *80*, 4204−4210.
(7) Guo, Y.; Smith, S. C.; Moore, C. B.; Melius, C. F. Kinetics and Product Branching Ratios for the Reaction HCO + NO_2. *J. Phys. Chem.* **1995**, *99*, 7473−7475.
(8) Lin, C.-Y.; Wang, H.-T.; Lin, M. C.; Melius, C. F. A Shock Tube Study of the CH_2O + NO_2 Reaction at High Temperatures. *Int. J. Chem. Kinet.* **1990**, *22*, 455−482.
(9) Rim, K. T.; Hershberger, J. F. Product Branching Ratios of the HCO + NO_2 Reaction. *J. Chem. Phys. A* **1998**, *102*, 5898−5902.
(10) Timonen, R. S.; Ratajczak, E.; Gutman, D. Kinetics of the Reactions of the Formyl Radical with Oxygen, Nitrogen Dioxide, Chlorine, and Bromine. *J. Chem. Phys.* **1988**, *92*, 651−655.
(11) Atkinson, R.; Finlayson, B. J.; Pitts, J. J. N. Photoionization Mass Spectrometer Studies of Gas Phase Ozone−Olefin Reactions. *J. Am. Chem. Soc.* **1973**, *95*, 7592−7599.
(12) Engdahl, A.; Nelander, B. A 1:1 Complex between a Hydroxyl Radical and Ozone. *J. Chem. Phys.* **2005**, *122*, 126101.
(13) Mansergas, A.; Anglada, J. M. Theoretical Characterization of the Gas-Phase O_3···HO Hydrogen-Bonded Complex. *ChemPhysChem* **2006**, *7*, 1488−1493.
(14) Mansergas, A.; Anglada, J. M. The Gas-Phase Hydrogen-Bonded Complex between Ozone and Hydroperoxyl Radical. A Theoretical Study. *J. Phys. Chem. A* **2007**, *111*, 976−981.
(15) Xu, Z. F.; Lin, M. C. Ab Initio Study on the Kinetics and Mechanisms for O_3 Reactions with HO_2 and HNO. *Chem. Phys. Lett.* **2007**, *440*, 12−18.
(16) Hansen, J. C.; Francisco, J. S. Radical−Molecule Complexes: Changing Our Perspective on the Molecular Mechanisms of Radical−Molecule Reactions and Their Impact on Atmospheric Chemistry. *ChemPhysChem* **2002**, *3*, 833−840.
(17) Turco, R. P.; Whitten, R. C.; Poppoff, I. G.; Capone, L. A. SSTs, Nitrogen Fertilizer and Stratospheric Ozone. *Nature* **1978**, *276*, 805−807.
(18) Whitten, R. C.; Borucki, W. J.; Capone, L. A.; Turco, R. P. Effect of the Reaction HO_2 + O_3 → OH + $2O_2$ on Stratospheric Ozone. *Nature* **1978**, *275*, 523−524.
(19) Varandas, A. J. C.; Zhang, L. Dynamics of HO_2 + O_3 Reaction Using a Test DMBE Potential Energy Surface: Does It Occur via Oxygen or Hydrogen Atom Abstraction? *Chem. Phys. Lett.* **2004**, *385*, 409−416.
(20) Viegas, L. P.; Varandas, A. J. C. HO_2 + O_3 Reaction: Ab Initio Study and Implications in Atmospheric Chemistry. *J. Chem. Theory Comput.* **2010**, *6*, 412−420.
(21) Klippenstein, S. J.; Wagner, A. F.; Dunbar, R. C.; Wardlaw, D. M.; Robertson, S. H. *VARIFLEX*, version 1.00; Argonne National Laboratory: Argonne, IL, 1999.
(22) Frisch, M. J.; Pople, J. A.; Binkley, J. S. Self-Consistent Molecular Orbital Methods 25. Supplementary Functions for Gaussian Basis Sets. *J. Chem. Phys.* **1984**, *80*, 3265−3269.
(23) Hehre, W. J.; Radom, L.; Schleyer, P. V. R.; Pople, J. A. *Ab Initio Molecular Orbital Theory*; John Wiley: New York, 1986.
(24) Becke, A. D. A New Mixing of Hartree-Fock and Local Density-Functional Theories. *J. Chem. Phys.* **1993**, *98*, 1372−1377.
(25) Pople, J. A.; Head-Gordon, M.; Raghavachari, K. Quadratic Configuration Interaction. A General Technique for Determining Electron Correlation Energies. *J. Chem. Phys.* **1987**, *87*, 5968−5975.
(26) Gonzalez, C.; Schlegel, H. B. Improved Algorithms for Reaction Path Following: Higher-Order Implicit Algorithms. *J. Phys. Chem.* **1989**, *90*, 2154−2161.
(27) Raghavachari, K.; Trucks, G. W.; Pople, J. A.; Head-Gordon, M. A Fifth-Order Perturbation Comparison of Electron Correlation Theories. *Chem. Phys. Lett.* **1989**, *157*, 479−483.
(28) Lee, T. J.; Taylor, P. R. A Diagnostic for Determining the Quality of Single-Reference Electron Correlation Methods. *Int. J. Quantum Chem. Symp.* **1989**, *23*, 199−207.
(29) Rienstra-Kiracofe, J. C.; Allen, W. D.; Schaefer, H. F., III. The C_2H_5 + O_2 Reaction Mechanism: High-Level Ab Initio Characterizations. *J. Phys. Chem. A* **2000**, *104*, 9823−9840.
(30) Knowles, P. J.; Werner, H.-J. An Efficient Second-Order MC SCF Method for Long Configuration Expansions. *Chem. Phys. Lett.* **1985**, *115*, 259−267.
(31) Roos, B. O.; Linse, P.; Siegbahn, P. E. M.; Blomberg, M. R. A. A Simple Method for the Evaluation of the Second-Order-Perturbation Energy from External Double-Excitations with a CASSCF Reference Wavefunction. *Chem. Phys.* **1982**, *66*, 197−207.
(32) Werner, H.-J.; Knowles, P. J. A Second Order Multiconfiguration SCF Procedure with Optimum Convergence. *J. Chem. Phys.* **1985**, *82*, 5053−5063.
(33) Celani, P.; Werner, H.-J. Multireference Perturbation Theory for Large Restricted and Selected Active Space Reference Wave Functions. *J. Chem. Phys.* **2000**, *112*, 5546−5557.
(34) Werner, H.-J. Third-Order Multiconfiguration Reference Perturbation Theory: The CASPT3 Method. *Mol. Phys.* **1996**, *89*, 645−661.
(35) Wolinski, K.; Pulay, P. Generalized Møller−Plesset Perturbation Theory: Second Order Results for Two-Configuration, Open-Shell Excited Singlet, and Doublet Wave Functions. *J. Chem. Phys.* **1989**, *90*, 3647−3659.
(36) Wolinski, K.; Sellers, H. L.; Pulay, P. Consistent Generalization of the Møller−Plesset Partitioning to Open-Shell and Multiconfigurational SCF Reference States in Many-Body Perturbation Theory. *Chem. Phys. Lett.* **1987**, *140*, 225−231.
(37) *NIST Computational Chemistry Comparison and Benchmark Database*, NIST Standard Reference Database Number 101, Release 15b. Johnson, R. D. Johnson, III, Ed. http://cccbdb.nist.gov/ (August 2011).